

Influence of Room-Temperature Ionic Liquids on the Electrosynthesis of CuBDC Type Metal-Organic Frameworks: Crystallite Size and Productivity

Laela Mukaromah, Yessi Permana, Aep Patah*

Received

23 September 2021

Received in revised form

14 March 2022

Accepted

15 March 2022

DOI: 10.5614/jrdn.2022.2.1.17142

The influence of imidazolium- and ammonium-based room-temperature ionic liquids (RTILs) i.e., [bmim][BF₄], [bmim][DCA], and MTBS, respectively, as electrolytes on the crystallite size and productivity of CuBDC (BDC=1,4-benzenedicarboxylate) type metal-organic frameworks (MOFs) by electrosynthesis method via anodic dissolution, was investigated. CuBDC was characterized by Fourier transform infrared spectroscopy (FTIR), powder X-ray diffraction (PXRD), thermogravimetric analysis (TGA), and nitrogen physisorption. The crystallite size and productivity of CuBDC using [bmim][BF₄], [bmim][DCA], MTBS as electrolytes were 24.7 nm, 22.1 nm, 20.5 nm, and 236 mg/h, 69 mg/h, 291 mg/h, respectively. The bulkier structure of ammonium-based RTILs resulted in CuBDC with a smaller crystallite size and higher productivity compared to imidazolium-based RTILs.

Keywords: RTILs; CuBDC; electrosynthesis; crystallite size; productivity.

Introduction

In the past decade, metal-organic frameworks (MOFs) have emerged as a promising class of crystalline materials in many applications with more than 81,000 structures reported in the Cambridge Structural Database (CSD). MOFs or porous coordination polymers (PCPs) are the third-generation porous material after carbon and zeolite constructed from metal ion clusters and organic linkers (Kitagawa et al., 2004). Owing to the high porosity, high thermal stability, large surface area, and pore volume, also feasible in structure modification or functionalization make these materials a good candidate, particularly in gas separation and storage applications (Anjum et al., 2015; Flaig et al., 2017; Oliveira et al., 2019).

Some types of MOFs, HKUST-1 and CuBDC, constructed from Cu²⁺ ions with 1,3,5-benzenetricarboxylate (BTC) and 1,4-benzenedicarboxylate (BDC) linkers, respectively, are known for having open metal sites (OMS) property, an unsaturated metal center which allows reversible coordination with Lewis base molecules, such as solvent (Chui et al., 1999; Mori et al., 1997). Both MOFs exhibit identical secondary building units (SBUs) of Cu₂(BDC)₂. HKUST-1 builds a three-dimensional pore system in paddle-wheel geometry, while CuBDC builds a two-dimensional pore system in lamellar geometry (Jeong et al., 2012; Kim et al., 2015).

To date, MOFs are commonly prepared using the conventional heating synthesis method that results in a good crystalline structure. However, this method involves high temperatures and long reaction times to enhance the formation of MOFs

(Chen et al., 2018). This reaction condition subsequently leads to an energy-inefficiency issue for the large-scale production of MOFs. Hence, the development of other alternative synthesis methods which can work at mild temperatures and short reaction times becomes necessary.

The electrosynthesis method of MOFs was first introduced by BASF Germany that successfully synthesized HKUST-1 at room temperature for 2.5 h (Mueller et al., 2006). In comparison, IRMOF-3 was reported at room temperature within 3 h synthesis (Wei et al., 2018). In this method, the source of metal ions was provided from metal plates via anodic dissolution by applying a specific voltage and current. Moreover, avoiding the use of metal salts which facilitates the formation of MOFs without impurities, such as nitrate or chloride is also an advantage of this method (Stock and Biswas, 2012). Nevertheless, due to the low conductivity of commonly used organic solvents, electrolytes are required to increase the conductivity of the solution in the electrosynthesis of MOFs.

In recent years, attention to room-temperature ionic liquids (RTILs) as electrolytes in various electrochemical applications has significantly increased. RTILs are liquid phase salts that show several excellent properties, such as high ionic conductivity, electrochemical and thermal stability, non-flammable, negligible vapor pressure, and good solubility (Fujie et al., 2015; Neto et al., 2014). The utilization of RTILs as electrolytes or solvents can direct the formation of a framework that affects the structure and morphology of MOF (Al-Kutubi et al., 2015; Sang et al., 2017). Tributylmethylammonium methyl sulfate (MTBS), the ammonium-based ionic liquid used in the electrosynthesis of ZIF-8 (zeolitic imidazolate frameworks) resulted in the highest Faraday efficiency of 81 % and productivity up to 250 mg/h (Martinez Joaristi et al., 2012). Electrosynthesis of MOF-5 with

Division of Inorganic and Physical Chemistry, Institut Teknologi Bandung, Jl. Ganesha No 10, Bandung 40132, Indonesia

* Corresponding author: aep@itb.ac.id

the addition of 1-butyl-3-methylimidazolium chloride [bmim][Cl] exhibited better crystallinity and higher thermal stability compared to the solvothermal method (Yang et al., 2015). Yet, the influence of various RTILs as electrolytes on the electrosynthesis of CuBDC had not been reported.

Herein, we reported the electrosynthesis of CuBDC type MOFs at room temperature and investigated the influence of RTILs on crystallite size and productivity. Imidazolium- and ammonium-based ionic liquids, namely 1-butyl-3-methylimidazolium tetrafluoroborate [bmim][BF₄], 1-butyl-3-methylimidazolium dicyanamide [bmim][DCA], and MTBS, respectively, were employed as electrolytes.

Experimental

Materials

All chemicals used were commercially available. Copper plates, Cu(NO₃)₂·3H₂O (Merck, ≥ 99.5 %), H₂BDC (Merck, ≥ 98 %), MTBS (Sigma-Aldrich, ≥ 95 %), [bmim][BF₄] (Iolitec, 99.5 %), [bmim][DCA] (Iolitec, > 98 %), DMF (Merck), methanol (Fulltime), and ethanol (Fulltime) were employed without further purification.

Synthesis of CuBDC

The electrosynthesis of CuBDC was modified from a previous report (Martinez Joaristi et al., 2012). MTBS (0.9344 g, 3 mmol) was dissolved in 30 mL of DMF under an inert atmosphere. H₂BDC (0.4984 g, 3 mmol) was added to DMF-MTBS solution and stirred until homogeneous. Before use, copper plates (1 cm x 5 cm) were mechanically polished with 240 and 600 grit sizes sandpapers, sonicated in ethanol for 5 min, dried, and weighed. Copper plates used as cathode and anode were separated by 2 cm. Electrosynthesis was conducted for 2 h at room temperature using a voltage of 10 V and a current density of 10 mA/cm². After solvent decantation, the product was soaked in 5 mL of methanol for 4 h and repeated three times. The product was then filtrated and labeled by as-synthesized CuBDC. The product was fully desolvated by vacuum heating at 200 °C for 6 h and labeled by degassed CuBDC. The range of voltages from 5 to 15 V and concentrations of 0.5 and 1 mmol RTILs/10 mL DMF were employed. Variation of electrolytes using imidazolium-based RTILs, namely [bmim][BF₄] and [bmim][DCA] was conducted at a voltage of 10 V and concentration of 1 mmol RTILs/10 mL DMF according to DMF-MTBS procedure.

The solvothermal synthesis of CuBDC was modified from a previous report (Carson et al., 2009). Cu(NO₃)₂·3H₂O (0.7248 g, 3 mmol) and H₂BDC (0.4984 g, 3 mmol) were dissolved in 30 ml of DMF, sonicated at room temperature for 30 min, then heated in an oven at 120 °C for 24 h. After cooled down at room temperature, the solvent was decanted. Solvent exchange and degassing processes were conducted with a similar procedure in the electrosynthesis method.

Characterization

Powder X-ray diffraction (PXRD) patterns were collected in the 2θ range of 5–50° using Rigaku MiniFlex 600 diffractometer with Cu-Kα radiation source (λ = 1.540593 Å). Thermogravimetric analysis (TGA) was carried out using NETZSCH STA 449 F3 Jupiter thermal analyzer in a temperature range of 20–500 °C with a heating rate of 20 °C/min under a nitrogen atmosphere. Fourier-transform infrared (FTIR) spectra were recorded on a Bruker Alpha instrument with a ZnSe beam splitter by dispersing the sample into a potassium bromide pellet. Nitrogen physisorption measurement was conducted using Quantachrome NOVAtouch 4LX analyzer at 77 K, and the sample was degassed at 225 °C for 6 h, before use.

Results and discussion

Synthesis of CuBDC

The electrosynthesis of CuBDC type MOFs was successfully conducted at room temperature for 2 h in the electrolyte/solvent system of 1 mmol MTBS/10 mL DMF to yield as-synthesized CuBDC as a Tosca powder. CuBDC revealed two different structures based on the coordination of DMF into the Cu²⁺ center. The structure of CuBDC with DMF coordination showed a monoclinic crystal system, while without DMF coordination showed a triclinic crystal system (Carson et al., 2009, 2014). The activation process of as-synthesized CuBDC at 200 °C for 6 h resulted in a dark blue powder of degassed CuBDC. The color change of CuBDC after the activation process indicates the loss of DMF coordination around the Cu²⁺ center giving a different crystal system as previously reported (Kim et al., 2015).

PXRD patterns of the as-synthesized CuBDC of the electrosynthesis and solvothermal methods show the characteristic peaks at 2θ of 10.08°, 17.02°, 24.70°, and 10.04°, 17.02°, 24.70°, respectively, that is by the previous report (Carson et al., 2009), as presented in Fig. 1. The as-synthesized CuBDC of the electrosynthesis method exhibits an identical relative intensity ratio to the solvothermal method.

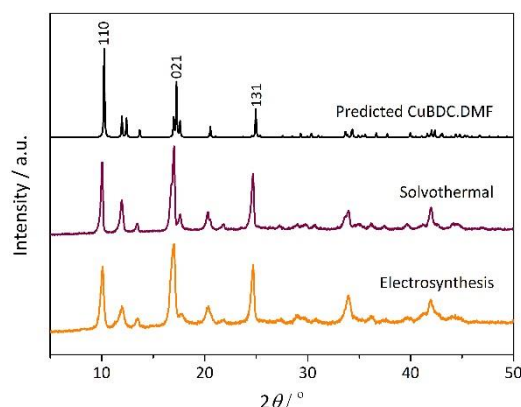


Figure 1. PXRD patterns of the as-synthesized CuBDC

This analysis explains that electrosynthesis is a promising method to produce CuBDC type MOFs. After the activation process, PXRD patterns of the degassed CuBDC of the electrosynthesis and solvothermal methods show characteristic peaks at 2θ of 8.22° , 9.00° , and 8.16° , 9.08° , respectively, which is also in agreement with the previous report (Carson et al., 2014), (Fig. S1). The degassed CuBDC of the electrosynthesis method reveals peaks with a higher relative intensity ratio in the 2θ range of $10\text{--}15^\circ$ compared to the solvothermal method. This result indicates the existence of the as-synthesized CuBDC phase in the degassed CuBDC. Therefore, a longer activation process is presumably required to completely remove the coordination of DMF in OMS and give a homogenous phase of the degassed CuBDC from the electrosynthesis method.

Variation of Voltages

Variation of voltages at 5, 10, and 15 V was applied in a 1 mmol MTBS/10 mL DMF electrolyte system. PXRD patterns of the as-synthesized CuBDC at a voltage of 5 V show a peak at 2θ of 10.23° with a lower relative intensity ratio than 10 and 15 V (Fig. S2). This analysis explains that the electrosynthesis of CuBDC conducted at a voltage of 10 and 15 V results in a more dominant crystal growth at the (110) plane. A peak shifting at 2θ of 17.26° of the as-synthesized CuBDC (5 V) is presumably related to the change of atomic arrangement in the crystal at the (021) plane. The crystallite size and productivity of the as-synthesized CuBDC at a voltage of 5, 10, and 15 V are 20.7 nm, 20.5 nm, 19.2 nm, and 77 mg/h, 291 mg/h, 295 mg/h, respectively, as shown in Fig. 2. An increase in voltage results in smaller crystallite size and higher productivity of CuBDC. Meanwhile, the productivity of CuBDC that does not significantly increase at a voltage of 15 V is very likely due to the applied voltage exceeding the electrochemical stability of MTBS. Therefore, the electrosynthesis of CuBDC in the 1 mmol MTBS/10 mL DMF electrolyte system is optimally conducted at a voltage of 10 V.

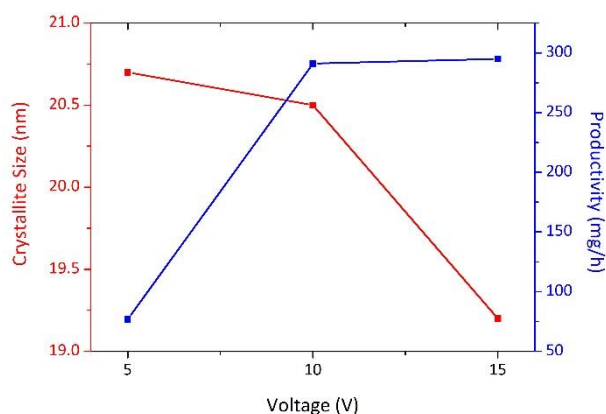


Figure 2. Crystallite size and productivity of the as-synthesized CuBDC at various voltages.

Variation of RTILs

Variation of RTILs was conducted according to a 1 mmol MTBS/10 mL DMF electrolyte system at a voltage of 10 V. The influence of RTILs i.e. [bmim][BF₄], [bmim][DCA], and MTBS on the electrosynthesis of CuBDC type MOFs was investigated. FTIR spectra of the as-synthesized CuBDC at various RTILs and H₂BDC are presented in Fig. 3. The shift of wavenumber of carbonyl group stretching vibration in BDC ligand is observed from 1680 cm^{-1} in a free ligand to 1667 cm^{-1} in CuBDC. The asymmetric stretching vibration of the carboxyl group is observed at 1630 cm^{-1} wavenumber. Furthermore, the shift of the wavenumber of the symmetric stretching vibration of the carboxyl group is also observed from 1425 cm^{-1} in a free ligand to 1397 cm^{-1} in CuBDC. This analysis explains that the BDC ligand is coordinated into the Cu²⁺ center to form the frameworks of CuBDC.

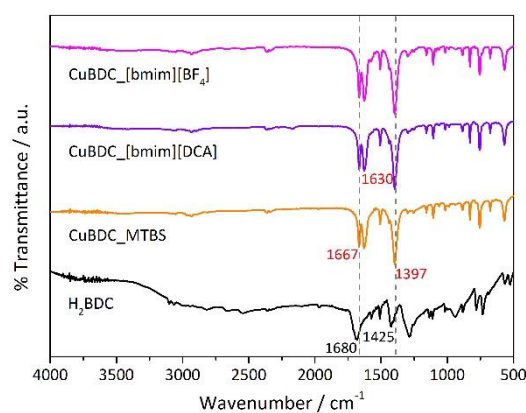


Figure 3. FTIR spectra of the as-synthesized CuBDC at various RTILs and H₂BDC.

PXRD patterns of the as-synthesized CuBDC at various RTILs are shown in Fig. 4. The as-synthesized CuBDC using [bmim][DCA] and [bmim][BF₄] as electrolytes exhibit a peak shifting at 2θ of 17.26° . This shifting is presumably due to the change of atomic arrangement in the crystal at the (021) plane, as observed in the as-synthesized CuBDC using MTBS at a voltage of 5 V. Meanwhile, the degassed CuBDC using [bmim][DCA] results peak with the lowest relative intensity ratio in the 2θ

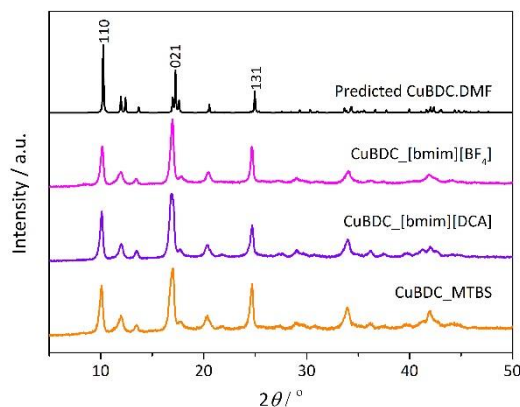


Figure 4. PXRD patterns of the as-synthesized CuBDC at various RTILs.

range of 10–15° corresponding to the as-synthesized CuBDC phase (Fig. S3). The density of [bmim][DCA] that is lower than [bmim][BF₄] and MTBS likely plays a role in reducing the coordination of DMF into OMS of CuBDC during the electrosynthesis process (Stoppa et al., 2010; Zech et al., 2010).

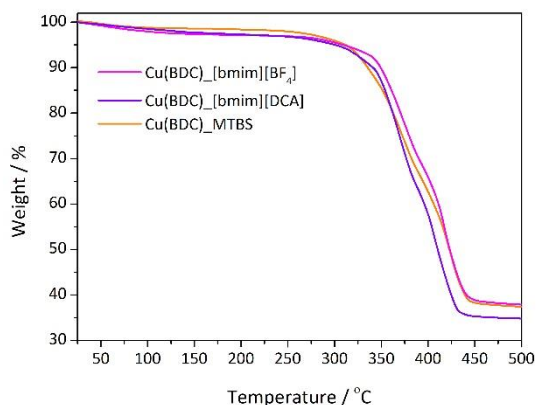


Figure 5. TGA profiles of the degassed CuBDC at various RTILs.

TGA profiles of the degassed CuBDC show no significant weight loss at temperatures below 300 °C, as presented in Fig. 5. The degassed CuBDC using [bmim][BF₄], [bmim][DCA], and MTBS RTILs as electrolytes exhibits thermal stability up to 325 °C, 310 °C, and 315 °C, respectively. The thermal stability of CuBDC using [bmim][BF₄] is identical to the reported solvothermal CuBDC (Carson et al., 2009). This analysis explains that the rapid nucleation that occurred in the electrosynthesis method of CuBDC does not lead to low thermal stability MOFs.

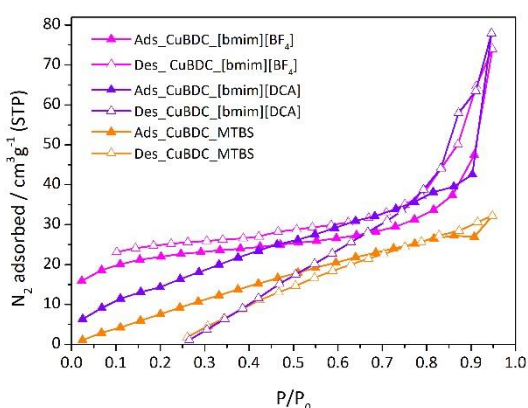


Figure 6. Isotherm curves of the degassed CuBDC at various RTILs.

Nitrogen physisorption measurement was conducted to determine the Brunauer-Emmett-Teller (BET) surface area of CuBDC type MOFs. BET surface area of the degassed CuBDC using [bmim][BF₄], [bmim][DCA], and MTBS RTILs as electrolytes is 72.8 m² g⁻¹, 60.5 m² g⁻¹, and 57.1 m² g⁻¹, respectively. The electrosynthesis of CuBDC exhibits a much lower surface area than reported solvothermal CuBDC, that is

625 m² g⁻¹ (Carson et al., 2009). The agglomeration of nano-sized crystallite presumably limits nitrogen access to fill the pore, resulting in MOFs with a low surface area (Furukawa et al., 2013). Isotherm curves of the degassed CuBDC are shown in Fig. 6.

The crystallite size and productivity of the as-synthesized CuBDC using electrosynthesis and solvothermal methods are compared. The crystallite size and productivity of the as-synthesized CuBDC using [bmim][BF₄], [bmim][DCA], and MTBS RTILs as electrolytes are 24.7 nm, 22.1 nm, 20.5 nm, and 236 mg/h, 69 mg/h, 291 mg/h, respectively. While the crystallite size and productivity of the as-synthesized CuBDC using the solvothermal method are 27.3 nm and 37 mg/h, respectively. Bulkier structure of ammonium-based RTILs (MTBS) results CuBDC with a smaller crystallite size and higher productivity compared to imidazolium-based RTILs ([bmim][BF₄], [bmim][DCA]). Furthermore, the electrosynthesis of CuBDC type MOFs can be conducted at room temperature and a shorter reaction time without anion competition in the reaction system by avoiding the use of metal salt.

Conclusions

The electrosynthesis of thermally stable CuBDC type MOFs was successfully conducted at room temperature for 2 h in various RTILs as electrolytes. The bulkier structure of ammonium-based RTILs (MTBS) results in smaller crystallite size and higher productivity compared to imidazolium-based RTILs ([bmim][BF₄], [bmim][DCA]) on the electrosynthesis of CuBDC.

Conflict of Interest

We have no conflict to declare.

Acknowledgments

LM acknowledges the Indonesia Endowment Fund for Education (LPDP) from the Ministry of Finance for the master program scholarship, and AP thanks Institut Teknologi Bandung through Riset ITB 2020 for research support.

References

- Al-Kutubi, H. *et al.* (2015) 'Electrosynthesis of metal-organic frameworks: Challenges and opportunities', *ChemElectroChem*, 2(4), pp. 462–474. doi: 10.1002/celec.201402429.
- Anjum, M. W. *et al.* (2015) 'Modulated UiO-66-based mixed-matrix membranes for CO₂ separation', *ACS Applied Materials and Interfaces*, 7(45), pp. 25193–25201. doi: 10.1021/acsami.5b08964.
- Carson, C. G. *et al.* (2014) 'Structure solution from powder diffraction of copper 1,4-benzenedicarboxylate', *European*

- Journal of Inorganic Chemistry*, 12, pp. 2140–2145. doi: 10.1002/ejic.201301543.
- Carson, C. G. *et al.* (2009) 'Synthesis and structure characterization of copper terephthalate metal-organic frameworks', *European Journal of Inorganic Chemistry*, 16, pp. 2338–2343. doi: 10.1002/ejic.200801224.
- Chen, Y. *et al.* (2018) 'Liquid-assisted mechanochemical synthesis of copper-based MOF-505 for the separation of CO₂ over CH₄ or N₂', *Industrial & Engineering Chemistry Research*, 57, pp. 703–709. doi: 10.1021/acs.iecr.7b03712.
- Chui, S. S.-Y. *et al.* (1999) 'A chemically functionalizable nanoporous material [Cu₃(TMA)₂(H₂O)₃]_n', *Science*, 283, pp. 1148–1150. doi: 10.1126/science.283.5405.1148.
- Flaig, R. W. *et al.* (2017) 'The chemistry of CO₂ capture in an amine-functionalized metal-organic framework under dry and humid conditions', *Journal of the American Chemical Society*, 139(35), pp. 12125–12128. doi: 10.1021/jacs.7b06382.
- Fujie, K. *et al.* (2015) 'Low temperature ionic conductor: Ionic liquid incorporated within a metal-organic framework', *Chemical Science*, 6(7), pp. 4306–4310. doi: 10.1039/c5sc01398d.
- Furukawa, H. *et al.* (2013) 'The chemistry and applications of metal-organic frameworks', *Science*, 341, p. 1230444. doi: 10.1126/science.1230444.
- Jeong, N. C. *et al.* (2012) 'Coordination-chemistry control of proton conductivity in the ionic metal-organic framework material HKUST-1', *Journal of the American Chemical Society*, 134(1), pp. 51–54. doi: 10.1021/ja2110152.
- Kim, H. K. *et al.* (2015) 'A chemical route to activation of open metal sites in the copper-based metal-organic framework materials HKUST-1 and Cu-MOF-2', *Journal of the American Chemical Society*, 137(31), pp. 10009–10015. doi: 10.1021/jacs.5b06637.
- Kitagawa, S., Kitaura, R., Noro, S. (2004) 'Functional porous coordination polymers', *Angewandte Chemie - International Edition*, 43(18), pp. 2334–2375. doi: 10.1002/anie.200300610.
- Martinez Joaristi, A. *et al.* (2012) 'Electrochemical synthesis of some archetypical Zn²⁺, Cu²⁺, and Al³⁺ metal organic frameworks', *Crystal Growth & Design*, 12(7), pp. 3489–3498. doi: 10.1021/cg300552w.
- Mori, W. *et al.* (1997) 'Synthesis of new adsorbent copper(II) terephthalate', *Chemistry Letters*, 26(12), pp. 1219–1220. doi: 10.1246/cl.1997.1219.
- Mueller, U. *et al.* (2006) 'Metal-organic frameworks - Prospective industrial applications', *Journal of Materials Chemistry*, 16(7), pp. 626–636. doi: 10.1039/b511962f.
- Neto, M. J. *et al.* (2014) 'Ionic liquids for solid-state electrolytes and electrosynthesis', *Journal of Electroanalytical Chemistry*, 714–715, pp. 63–69. doi: 10.1016/j.jelechem.2013.12.013.
- Oliveira, L. T. *et al.* (2019) 'Superior performance of mesoporous MOF MIL-100 (Fe) impregnated with ionic liquids for CO₂ adsorption', *Journal of Chemical & Engineering Data*, 64(5), pp. 2221–2228. doi: 10.1021/acs.jced.8b01177.
- Sang, X. *et al.* (2017) 'Ionic liquid accelerates the crystallization of Zr-based metal-organic frameworks', *Nature Communications*, 8(1), pp. 1–7. doi: 10.1038/s41467-017-00226-y.
- Stock, N., Biswas, S. (2012) 'Synthesis of metal-organic frameworks (MOFs): Routes to various MOF topologies, morphologies, and composites', *Chemical Reviews*, 112(2), pp. 933–969. doi: 10.1021/cr200304e.
- Stoppa, A. *et al.* (2010) 'The conductivity of imidazolium-based ionic liquids from (-35 to 195) °C. A. variation of cations alkyl chain', *Journal of Chemical & Engineering Data*, 55(5), pp. 1768–1773. doi: 10.1021/je900793r.
- Wei, J.-Z. *et al.* (2018) 'Rapid and large-scale synthesis of IRMOF-3 by electrochemistry method with enhanced fluorescence detection performance for TNP', *Inorganic Chemistry*, 57(7), pp. 3818–3824. doi: 10.1021/acs.inorgchem.7b03174.
- Yang, H. *et al.* (2015) 'In situ electrochemical synthesis of MOF-5 and its application in improving photocatalytic activity of BiOBr', *Transactions of Nonferrous Metals Society of China (English Edition)*, 25(12), pp. 3987–3994. doi: 10.1016/S1003-6326(15)64047-X.
- Zech, O. *et al.* (2010) 'The conductivity of imidazolium-based ionic liquids from (248 to 468) K. B. variation of the anion', *Journal of Chemical & Engineering Data*, 55(5), pp. 1774–1778. doi: 10.1021/je900789j.